

Article

Artificial Neural Network for the Prediction of Fatigue Life of Microscale Single-Crystal Copper

Fanming Zeng^{1,2} and Yabin Yan^{1,2,*} 

¹ School of Mechanical Power and Engineering, East China University of Science and Technology, Shanghai 200237, China

² Shanghai Key Laboratory of Intelligent Sensing and Detection Technology, East China University of Science and Technology, Shanghai 200237, China

* Correspondence: yanyabin@ecust.edu.cn

Abstract: Microscale single-crystal copper is widely used in electronics, communications and other fields due to its excellent properties such as high ductility, high toughness and good conductivity. Therefore, it is particularly important to research its fatigue life. In order to explore the influence of size effect, loading frequency and shear strain on the main slip surface on the fatigue life of microscale single-crystal copper based on in situ fatigue experimental data of microscale single-crystal copper, this paper used a BP neural network algorithm to construct a single-crystal copper fatigue life prediction network model. The data set included 14 groups of training data, with 11 groups as training sets and 3 groups as testing sets. The input characteristics were length, width, height, loading frequency and shear strain of the main sliding plane of a microscale single-crystal copper sample. The output characteristic was the fatigue life of microscale single-crystal copper. After training, the mean square error (MSE) of the model was 0.03, the absolute value error (MAE) was 0.125, and the correlation coefficient (R^2) was 0.93271, indicating that the BP neural network algorithm can effectively predict the fatigue life of microscale single-crystal copper and has good generalization ability. This model can not only save the experimental time of fatigue life measurement of micro-scale single-crystal copper, but also optimize the properties of the material by taking equidistant points in the range of characteristic parameters. Therefore, the current study demonstrates an applicable and efficient methodology to evaluate the fatigue life of microscale materials in industrial applications.



Citation: Zeng, F.; Yan, Y. Artificial Neural Network for the Prediction of Fatigue Life of Microscale Single-Crystal Copper. *Crystals* **2023**, *13*, 539. <https://doi.org/10.3390/cryst13030539>

Academic Editor: Tomasz Sadowski

Received: 22 February 2023

Revised: 9 March 2023

Accepted: 10 March 2023

Published: 21 March 2023



Copyright: © 2023 by the authors. Licensee MDPI, Basel, Switzerland. This article is an open access article distributed under the terms and conditions of the Creative Commons Attribution (CC BY) license (<https://creativecommons.org/licenses/by/4.0/>).

Keywords: microscale single-crystal copper; BP neural network; fatigue life

1. Introduction

In recent years, with the rapid development of the electronic industry and communication technology, the industry has put forward higher requirements on the performance of conductors [1]. Under the development trend of integration and miniaturization of microelectronic components, the mechanical properties, microstructure, fatigue creep process and failure modes of micro-scale materials have become important research topics [2], especially the fatigue life of materials, which has become a considerable research direction. Due to its special crystal structure, there is no transverse grain boundary in single-crystal copper, which eliminates the resistance generation source and signal attenuation source so that it has good conductivity and signal transmission performance [3,4]. At the same time, it also has high ductility, easy processing, high purity and high toughness. It is widely used in electronics, communications, audio and other fields [5]. Moreover, with the emergence of technologies and instruments such as focused ion beam (FIB) and electron microscopes, it is possible to study the fatigue life of micron-sized single-crystal copper [6–8].

D. Kiener et al. [9] proposed an in situ test method for micro-tensile specimens. Load was along the direction of $\langle -2\ 3\ 4 \rangle$ of the samples. The diameter was between 0.5 μm and 8 μm , and aspect ratio, gauge length, and side length all ranged from 1:1 to 13.5:1. The

results show that the flow stress increases with the decrease in pipe diameter. When the diameter was more than 2 μm , the increase was small, and when it was less than 2 μm , it was slightly larger. These phenomena can be explained by plastic deformation mechanisms controlled by individual dislocation sources, but the phenomenon is significantly different when the aspect ratio is low. Obvious hardening and very strong size effects were observed. Yan et al. [10] analyzed and observed the shear stress change on the main slip surface of $1 \times 1 \times 2 \mu\text{m}$ single-crystal copper and the corresponding evolution of crystal slip in each period. Finally, the fatigue curve of micro single-crystal copper was obtained. The fatigue life obviously depended on the strain amplitude and is not sensitive to the frequency of cyclic loading. In addition, the fatigue life of micro-scale single-crystal copper is much shorter than that of bulk copper, revealing the strain dependence of the size effect of the fatigue life of micro-scale single-crystal copper. Kai Huang et al. [11] carried out a series of complete reverse tensile compression fatigue tests through constant displacement, including field observation. It was found that the load amplitude significantly affected the formation of early extrusion. A lower load threshold for crack initiation was observed. Above the load threshold, no significant load dependence of fatigue crack initiation was observed. Takashi Sumigawa et al. [12,13] carried out fatigue tests on single-crystal copper micron specimens under constant displacement amplitude. It was observed by SEM that strain localization caused by slip bands led to nanoscale extrusion/invasion on the surface, and crystal slip only occurred near the localized bands in continuous cycles. These phenomena indicate that the fatigue process of metals at microscale is different from that of bulk metals, as no characteristic dislocation substructure was formed during extrusion. Therefore, extrusion/invasion leads to fatigue failure in microscopic metals. These studies show that the fatigue life of microscale single-crystal copper is affected by size effect, loading frequency and shear stress on the main slip plane.

Machine learning is a multidisciplinary subject involving probability theory, statistics, approximation theory, convex analysis, algorithm complexity theory and many other subjects. It can directly use historical data to constantly adjust parameters in the model, optimize the model, and learn rules between data without the need to study and analyze potential physical mechanisms [14]. Driven by Big Data technology, machine learning algorithms have been widely used in the performance prediction and optimization of metals, alloys, polymers and other materials [15–17]. For alloy materials, M. Mesbah et al. [18] used radial basis function (RBF) and multilayer perceptron (MLP) artificial neural networks to train the mechanical property data of ZK60 magnesium alloy treated by ptcap and compared the predicted results of their neural networks with the experimental microscopic analysis results. It was found that both RBF and MLP can be used to accurately estimate the mechanical properties of ZK60 magnesium alloys treated with ptcap. Liu, HD et al. [14] established an analysis and prediction model of the correlation between the composition and mechanical properties of Mg-Al-Zn (AZ) magnesium alloys by using ANN. This model is based on a multi-layer feedforward neural network, which has good performance and can be used to simulate and predict the mechanical properties of AZ series magnesium alloys as a function of composition. Sun, Y et al. [19] developed and trained a backpropagation neural network (BP neural network) using data from published sources in the literature to investigate the effects of aluminum, molybdenum and zirconium on the β transition temperature of titanium alloys. The predicted results are in good agreement with the experimental results. For alloy metals, Maohua Li et al. [20] used an adaptive neurofuzzy reasoning system (ANFIS) and support vector machine (SVM) to determine the relationship between SPD parameters such as metal forming process type, pass and process temperature. Gene expression programming (GEP) and genetic programming (GP) were used to further validate the estimation capabilities of neuro-based predictive machine learning. The results show that the ANFIS and SVM algorithms can predict the mechanical behavior of UFG magnesium alloy well. For copper, Mayer, AE et al. [15] used ANNs, artificial neural networks (ANNs) trained with molecular dynamics (MDs) data, to predict the stress–strain relationship, shear modulus and generalized stratification of

single-crystal copper in the elastic stage before dislocation nucleation in a wide range of pressures from -10 GPa to $+50$ GPa. In addition, when preparing training data, polynomial extrapolation was carried out on MD data to exceed the nucleation limit and improve the training accuracy. Li, B et al. [16] derived the constitutive equation of copper pipe and established the dynamic recrystallization and grain growth model of copper pipe. The grain distribution of copper pipe was obtained by combining the microstructure evolution model with finite element simulation. The model used an artificial neural network to predict the grain size of copper pipe under different parameters and could be used to optimize the properties of rolled copper pipe. For nanomaterials, Yan et al. [21] modeled the physical and chemical properties and biological effects of six groups of gold nanoparticles by using a stochastic forest and a KNN algorithm. The model for the external test set predicted R^2 between 0.76 and 0.95. This study provided a new idea for the development of nanomaterial descriptors. In addition, in order to overcome the problem of insufficient descriptors of nanomaterials, Yan et al. [22] used CNNs to model and analyze images of nanomaterials and established prediction models of physical and chemical properties (logP and Zeta potential) and biological effects (cell uptake and protein adsorption) of nanomaterials. $R^2 > 0.68$ was used for cross-validation of all endpoints and the prediction effect of external data. With the progress of microscale experimental studies, the library of microscale material properties is gradually expanded. However, the application of ML methods on the prediction of fatigue life for microscale single-crystal copper still remains for further investigation.

Based on the fatigue data of single-crystal copper [10], this paper uses a BP artificial neural network algorithm to predict the length, width, height, loading frequency and shear strain of the main slip plane of single-crystal copper as the characteristic parameters, with the fatigue life as the label parameter.

2. Materials and Methods

2.1. BP Artificial Neural Network

Based on the polysynaptic transmission of human neurons, an artificial neuron was developed, which allows multiple inputs and gives results based on connection weights (W_i) and thresholds (b). The working principle of neurons is shown in Figure 1.

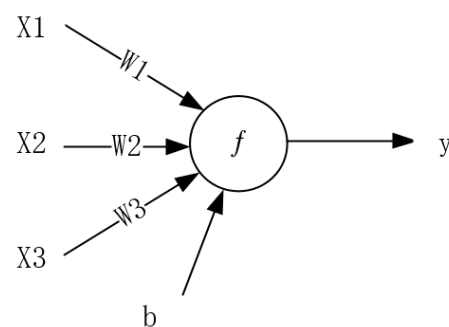


Figure 1. Working principle of neurons.

This model can be calculated by Equation (1).

$$y = f\left(\sum_{i=1}^n w_i x_i - b\right) \quad (1)$$

where y is the output, w_i is the weight of the neuron, x_i is the input data, b is the threshold, and f is the activation function.

The common activation functions are relu, sigmoid, tanh and other functions [23,24]. First, the weights are multiplied by the input data matrix and subtracted from the bias. Then, the result is substituted into the activation function to output the final result. According to the different activation functions, it can be used to solve the classification and regression

problems. Since the data in this paper are continuous and belong to the regression problem, the network uses the sigmoid and relu functions as the activation functions.

The sigmoid function can be calculated by Equation (2).

$$f(x) = \frac{1}{1 + e^{-x}} \quad (2)$$

The relu function can be calculated by Equation (3).

$$f(x) = \max(0, x) \quad (3)$$

When multiple neurons are added to the model, an artificial neural network is formed. The model connection principle diagram is shown in Figure 2. The input vector is $X = (X_1, X_2, \dots, X_5) T$, where X_1, X_2, X_3, X_4 and X_5 are the length, width, height and loading frequency and shear strain of the main slip plane of microscale single-crystal copper. The hidden layer output vector is $Y = (Y_1, Y_2, \dots, Y_m) T$. O_1 is the output vector representing the fatigue life. $V = (V_1, V_2, \dots, V_m) T$ is the weight matrix between the input layer and the hidden layer. $W = (W_1, W_2, \dots, W_k) T$ is the weight matrix between the hidden layer and the output layer. X_0 is the threshold set from the input layer to the hidden layer. Y_0 is the threshold set from the hidden layer to the output layer.

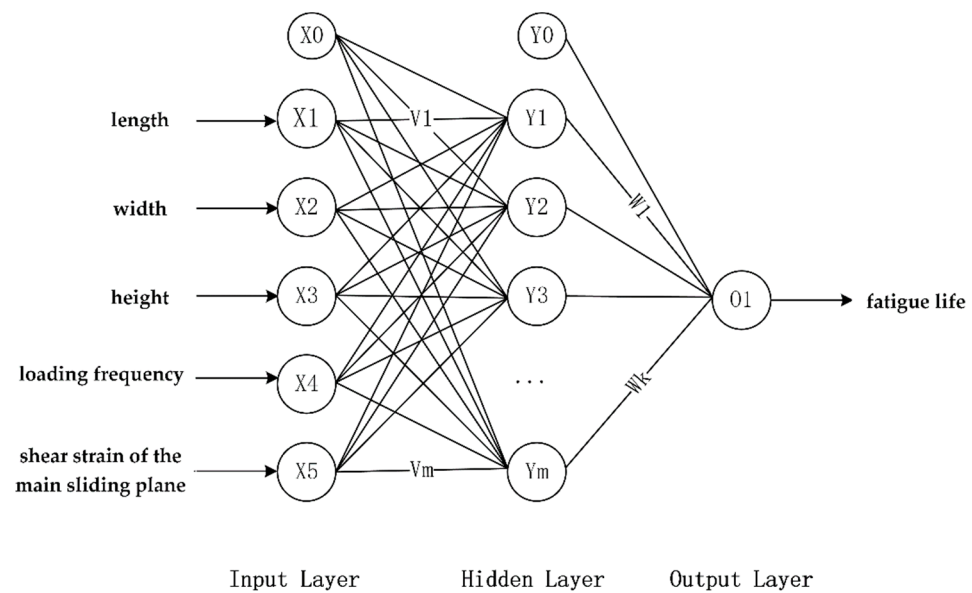


Figure 2. Model connection principle diagram.

The complete neural network model includes an input layer, an output layer and hidden layers. The first layer is the input layer. The training data are first imported into the input layer to directly determine the number of neurons in the input layer. The middle layers are hidden layers, and multiple hidden layers can be contained. Generally speaking, the hidden layer determines the complexity of the model and the training accuracy. The more neurons, the more complex the network, the higher the training accuracy. The final layer is the output layer of the model. For classification problems, the number of neurons is the same as the number of categories, and for regression problems, the number of neurons is the same as the number of label parameters. The connection between layers of neural network is generally full connection. That is, all neurons in the upper layer and all neurons in the lower layer are connected.

The BP neural network realizes the training of the model through the forward propagation of the data and the back propagation of the error. In the artificial neural network model, the loss function is used as the criterion for the completion of model training. Mean

square error (MSE) is often used as a loss function when solving regression problems. The mean square error can be calculated by Equation (4).

$$E = \frac{1}{n} \sum_{i=1}^n (f(x_i) - y_i)^2 \quad (4)$$

Among them, n is the total number of sample data, y_i is the true value of the samples, $f(x_i)$ is the predicted value of the samples.

The gradient descent method (SGD) is commonly used in back propagation; according to the value of the error function, the network weights and thresholds are constantly adjusted, and the loss function is iteratively optimized [25,26]. In this process, the parameters such as weights and bias are constantly updated, the value of the loss function is constantly changing, and the overall trend is decreasing. When a certain value is reached, the training is completed.

The weights and thresholds adjustment formulas are shown in Equations (5) and (6).

$$w(k+1) = w(k) - \alpha \frac{\partial E(k)}{\partial w(k)} \quad (5)$$

$$b(k+1) = b(k) - \alpha \frac{\partial E(k)}{\partial b(k)} \quad (6)$$

Among them, $w(k), b(k)$ are the weights and thresholds for the k th iteration in the network, $\frac{\partial E(k)}{\partial w(k)}, \frac{\partial E(k)}{\partial b(k)}$ are the error gradient of the output error to the weights and thresholds for the k th iteration, and α is the learning rate, which controls the iteration speed.

2.2. Experimental Data

The experimental data used in this paper came from Reference [10]. There were 14 groups of data, including 5 input features and 1 output feature, 11 sets as training sets and 3 sets as testing sets. The input features were the length, width, height, loading frequency, and shear strain on the main slip surface of the microscale single-crystal copper sample. The output feature was the fatigue life of the microscale single-crystal copper. Essentially, machine learning allows computers to learn the potential relationships in data and make predictions about future data based on those relationships. Therefore, data are very important for the accuracy of the algorithm. The quality of the data set matters more than the quantity. If the relationships between large data sets are fuzzy, chaotic data will mislead the algorithm, and it is difficult for the model to converge and learn the patterns from the training. When the relationship between small data sets is clear, it is easier for the algorithm to learn the patterns and it has higher prediction accuracy. Since the fatigue life values of single-crystal copper differ greatly under different experimental conditions, logarithmic processing was performed on the training data to narrow the gap between them. This method can not only accelerate the convergence speed of the model, but also improve the accuracy of the model.

2.3. Data Normalization

Normalization is a method of data processing in which all input parameters are expressed in the same unit, scaling the data to a common scale or range, keeping the dimensions the same. On the one hand, by assigning equal weights to all feature parameters in this way, the comparison and aggregation process among feature parameters can be simplified, and the convergence speed of model training can be improved, so that one feature parameter will not override other feature parameters. On the other hand, data normalization is helpful to prevent the machine learning algorithm using the distance measurement between characteristic parameters to produce distorted results, and can improve the efficiency of data analysis. Therefore, normalization becomes an efficient

data processing method. The most common data normalization methods are Z-Score and Min–Max [27,28].

Due to the large magnitude difference between the feature data and the label data used in this chapter, the gradient descent method was used to solve for the optimal value, which requires more iteration steps to converge. In order to improve the speed of model convergence and improve the accuracy of training without changing the data distribution, Min–Max normalization processing was performed on the data. The calculation method is shown in Equation (7):

$$x^* = \frac{x - x_{min}}{x_{max} - x_{min}} \quad (7)$$

where x_{min} is the minimum value in the data and x_{max} is the maximum value in the data.

The normalized data values are between 0 and 1.

2.4. Training Process

After obtaining the experimental data, the data were divided into training set and test set, and then the training set was input into the neural network to train the model. Finally, the accuracy of the trained network was tested using the test set. The training flow chart is shown in Figure 3.

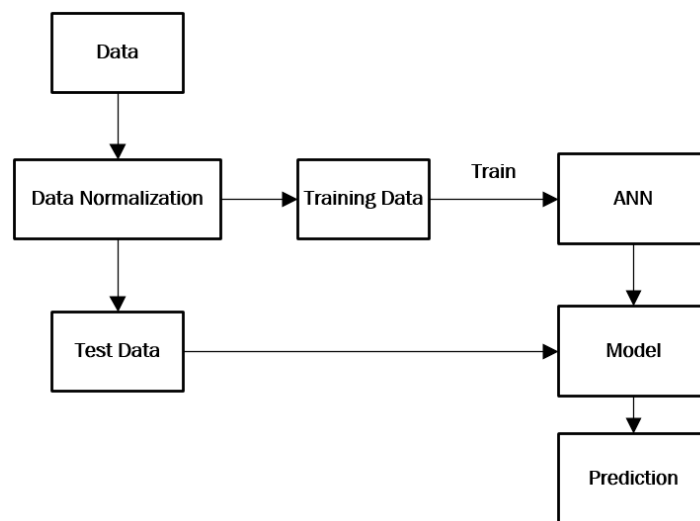


Figure 3. Training flow chart.

3. Results and Discussion

Tensorflow2.0 is a mature machine learning framework. This paper built an BP artificial neural network framework based on Keras in tensorflow2.0. The artificial neural network set up a five-layer network. The first layer is the straightening layer, which was used to process data and convert multi-dimensional input parameters into one-dimensional parameters. The remaining four layers are the dense layer, which is the main parameter layer of the model. The second layer was set up with 100 neurons, the third layer was set up with 50 neurons, and the fourth layer was set up with 18 neurons. All of them used the relu activation function and the L2 regularization method. Since the network output feature was fatigue life, there was one neuron in the last layer, namely the output layer. The sigmoid activation function was used and the L2 regularization method was used. The optimizer selected SGD and the learning rate of 0.03, and the loss function used mean square error. The input features of the model were the three-dimensional size of the microscale single-crystal copper, the loading frequency and the shear stress on the main slip surface. The output feature was the fatigue life. Before the data were imported into the model, the data were normalized first, then the sequence was disordered and randomly divided into test sets and training sets to improve the generalization ability of the model.

Mean square error, absolute value error and correlation coefficient R^2 were selected as accuracy measurement indexes.

The absolute value error can be calculated by Equation (8).

$$MAE = \frac{1}{n} \sum_{i=1}^n |f(x_i) - y_i| \quad (8)$$

The correlation coefficient R^2 can be calculated by Equation (9).

$$R^2 = 1 - \frac{\sum_{i=1}^n (y_i - f(x_i))^2}{\sum_{i=1}^n (y_i - \bar{y})^2} \quad (9)$$

where \bar{y} is the average of the predicted value.

According to the Equations (4), (8) and (9), the smaller the mean square error and absolute value error, the closer the predicted value and the true value, the higher the prediction accuracy of the model. The value range of R^2 is between 0 and 1. When it is closer to 1, it shows that the model has higher accuracy; when it is closer to 0, the greater the gap between the predicted value and the real value and the lower the accuracy.

The change in mean square error and absolute value error in the training process are shown in Figure 4. From the mean square error function curve, it can be seen that when the number of iterations was from 0 to 400 steps, the mean square error function value of the training set decreased from 0.148 to 0.02, the mean square error function value of the test set decreased from 0.143 to 0.03, the absolute value error function value of the training set decreased from 0.300 to 0.08, and the mean square error function value of the test set decreased from 0.255 to 0.125; in addition, the decrease speed was very fast. At this time, the parameter iteration was coarsely adjusted with the gradient decrease. During the training process from 400 steps to 3000 steps, the mean square error and absolute value error of the test set and the training set increased slightly, but the increase was not obvious. At this time, the parameter iteration was fine-tuned with the gradient descent. In the training process of 3000 steps to 5000 steps, the mean square error and absolute value error of the test set and the training set tended to be stable, and there was no obvious fluctuation.

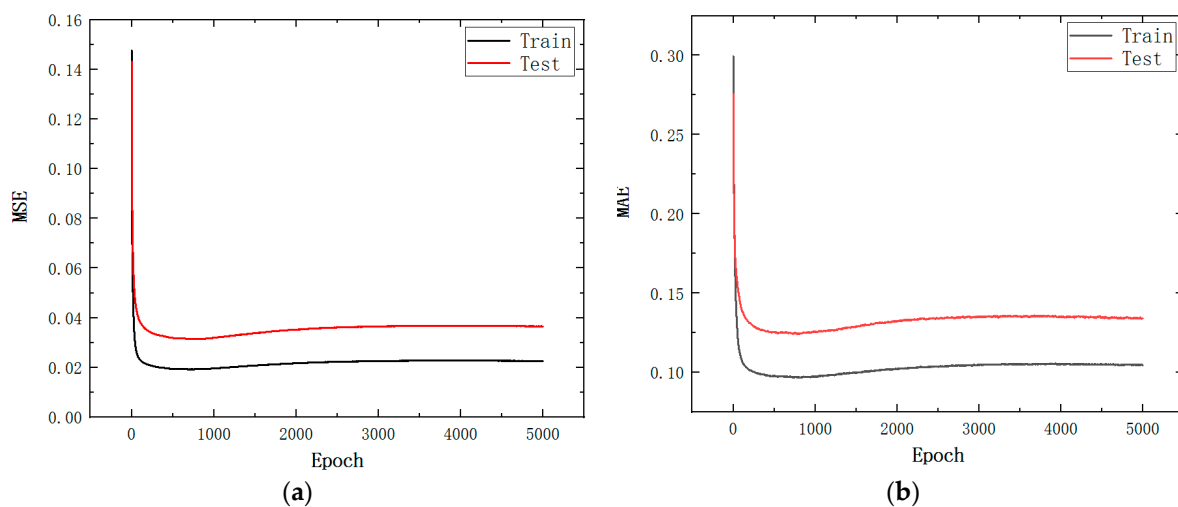


Figure 4. The function changes during training. (a) Mean square error. (b) Absolute value error variation.

The adjustment of each weight and bias term in the model was completed, and the training process was completed. The ideal mean square error value and absolute value

error value were obtained and indicated that the real value and the predicted value are similar. The model has high prediction accuracy and good generalization ability.

The prediction regression diagram shows a comparison of the predicted output results during the training process with the experimental objectives of the artificial neural network. Ideally, the output is the same as the objective of the artificial neural network. The slope of the regression diagram should be 1, the intercept should be 0, and the correlation coefficient of the ideal fitting is 1. The regression plots for the model predicting fatigue life are shown in Figure 5. Figure 5a shows the regression diagram of the training set. The slope of the line is 1.00122, the intercept is 0.07105, and the correlation coefficient R^2 reaches 0.94212. Figure 5b shows the regression diagram of the test set. The slope of the line is 0.94831, the intercept is 0.02139, and the correlation coefficient R^2 reaches 0.93271. Figure 5c shows the regression diagram of all sets. The slope of the line is 0.97967, the intercept is 0.08886, and the correlation coefficient R^2 reaches 0.9352. The fitting line and correlation of training set and test set are very close to 1. This indicates that the predicted fatigue life is similar to the experimental fatigue life.

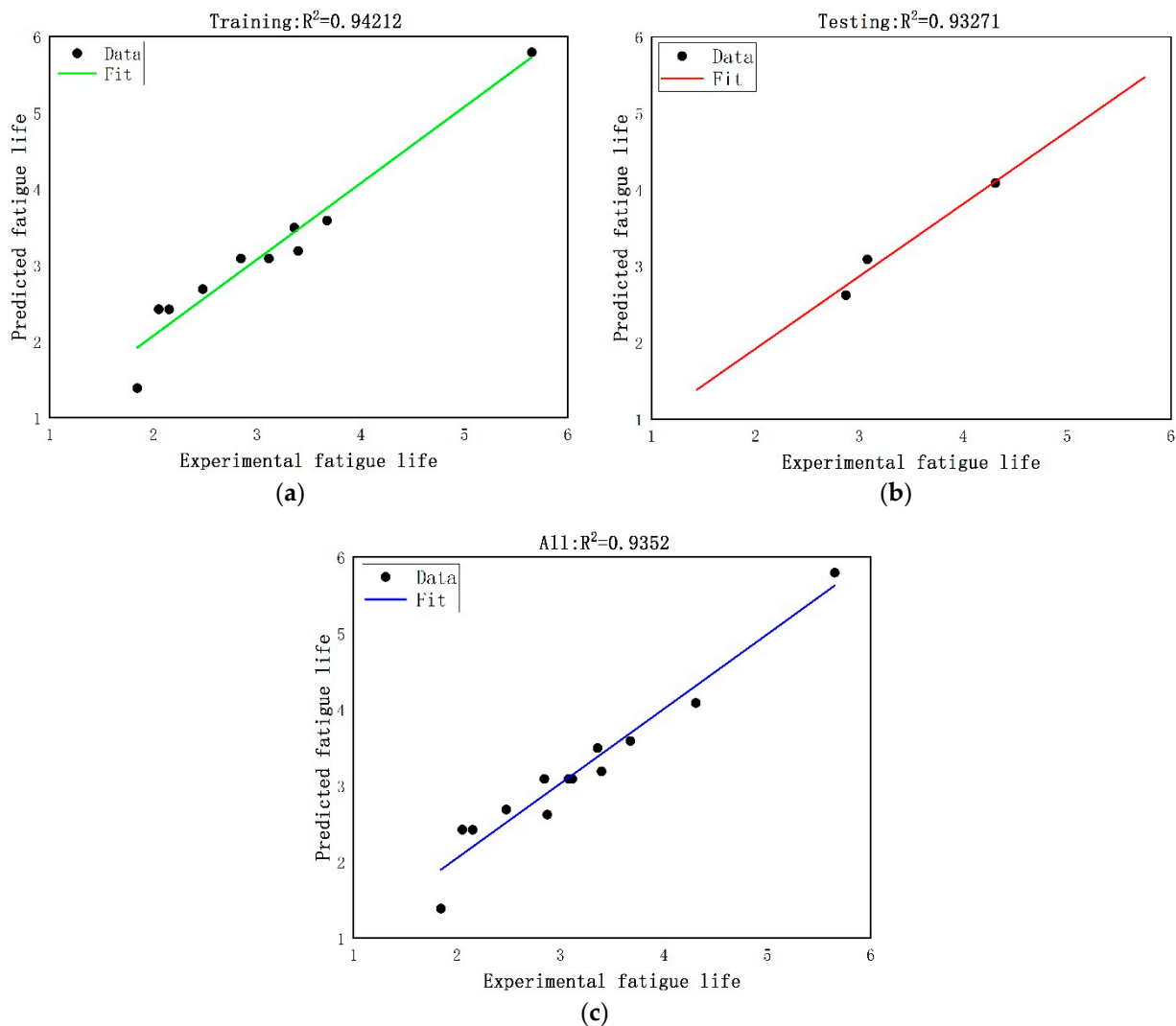


Figure 5. The regression plots for the model predicting fatigue life. (a) Training data. (b) Testing data. (c) All data.

The experimental value and the predicted value of the fatigue life of the microscale single-crystal copper are shown in Figure 6. The experimental value and the predicted value are highly coincident, which reflects the degree of model training and has good

generalization ability, indicating that the artificial neural network model has high accuracy for fatigue life prediction.

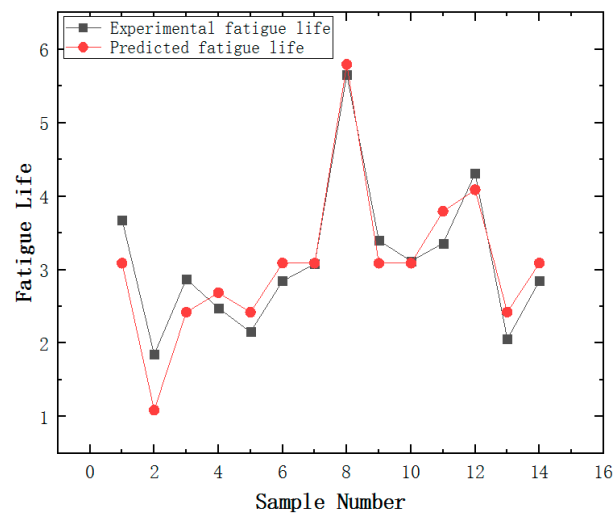


Figure 6. Comparison of experimental value and predicted value.

4. Conclusions

The results of this paper show that the prediction model using artificial neural network algorithm, three-dimensional size, loading frequency, shear strain on the main slip surface as the characteristic parameters, and fatigue life as the label parameter has high accuracy. The mean square error of the testing sets is 0.03, the absolute value error is 0.125, and the R^2 is 0.93271. The real fatigue life and the predicted fatigue life have a high coincidence. This technology has a good application prospect in the research field and industrial production. On the one hand, when the values of the input characteristic parameters are known, the fatigue life of microscale single-crystal copper can be effectively predicted by this prediction model, which can not only shorten the experimental measurement time and reduce the measurement cost, but also can be compared with the in situ experimental measurement results of fatigue of single-crystal copper. On the other hand, the orthogonal feature space can be formed by taking equidistant points of the feature parameters in the range, and then the new feature space can be imported into the prediction model to find the optimal fatigue life in the output results. This algorithm can effectively realize the performance optimization of microscale single-crystal copper.

Author Contributions: Writing—first draft preparation, conceptualization, methodology, data collection, building models, visualization, validation, F.Z.; Writing—review and editing, supervision, Y.Y. All authors have read and agreed to the published version of the manuscript.

Funding: This work was supported by the Natural Science Foundation of Shanghai (Grant No. 19ZR1413200).

Data Availability Statement: The data presented in this study are available on request from the corresponding author.

Conflicts of Interest: The authors declare no conflict of interest.

References

1. Chung, D.D.L.; Xi, X. A review of the colossal permittivity of electronic conductors, specifically metals and carbons. *Mater. Res. Bull.* **2022**, *148*, 111654. [[CrossRef](#)]
2. Liu, M.; Li, X. Mechanical properties measurement of materials and devices at micro- and nano-scale by optical methods: A review. *Opt. Lasers Eng.* **2022**, *150*, 106853. [[CrossRef](#)]
3. Singh, S.; Gangwar, S.; Yadav, S. A Review on Mechanical and Tribological Properties of Micro/Nano Filled Metal Alloy Composites. *Mater. Today Proc.* **2017**, *4*, 5583–5592. [[CrossRef](#)]

4. Sun, L.G.; Wu, G.; Wang, Q.; Lu, J. Nanostructural metallic materials: Structures and mechanical properties. *Mater. Today* **2020**, *38*, 114–135. [[CrossRef](#)]
5. Huang, K.; Sumigawa, T.; Kitamura, T. Experimental evaluation of loading mode effect on plasticity of microscale single-crystal copper. *Mater. Sci. Eng. A* **2021**, *806*, 140822. [[CrossRef](#)]
6. Gao, Z.; Hu, R.; Gao, X.; Wu, Y.; Zou, H.; Li, J.; Zhou, M. Characterization of the Widmanstätten structure in γ -TiAl alloy using an EBSD-FIB-TEM combined process. *Scr. Mater.* **2023**, *222*, 115001. [[CrossRef](#)]
7. Salvati, E.; O'Connor, S.; Sui, T.; Nowell, D.; Korsunsky, A.M. A study of overload effect on fatigue crack propagation using EBSD, FIB-DIC and FEM methods. *Eng. Fract. Mech.* **2016**, *167*, 210–223. [[CrossRef](#)]
8. Wilkinson, A.J.; Britton, T.B. Strains, planes, and EBSD in materials science. *Mater. Today* **2012**, *15*, 366–376. [[CrossRef](#)]
9. Kiener, D.; Grosinger, W.; Dehm, G.; Pippan, R. A further step towards an understanding of size-dependent crystal plasticity: In situ tension experiments of miniaturized single-crystal copper samples. *Acta Mater.* **2008**, *56*, 580–592. [[CrossRef](#)]
10. Yan, Y.; Sumigawa, T.; Wang, X.; Chen, W.; Xuan, F.; Kitamura, T. Fatigue curve of microscale single-crystal copper: An in situ SEM tension-compression study. *Int. J. Mech. Sci.* **2020**, *171*, 105361. [[CrossRef](#)]
11. Huang, K.; Sumigawa, T.; Kitamura, T. Load-dependency of damage process in tension-compression fatigue of microscale single-crystal copper. *Int. J. Fatigue* **2020**, *133*, 105415. [[CrossRef](#)]
12. Sumigawa, T.; Byungwoon, K.; Mizuno, Y.; Morimura, T.; Kitamura, T. In situ observation on formation process of nanoscale cracking during tension-compression fatigue of single crystal copper micron-scale specimen. *Acta Mater.* **2018**, *153*, 270–278. [[CrossRef](#)]
13. Sumigawa, T.; Uegaki, S.; Yukishita, T.; Arai, S.; Takahashi, Y.; Kitamura, T. FE-SEM in situ observation of damage evolution in tension-compression fatigue of micro-sized single-crystal copper. *Mater. Sci. Eng. A* **2019**, *764*, 138218. [[CrossRef](#)]
14. Liu, H.; Tang, A.; Pan, F.; Zuo, R.; Wang, L. A model on the correlation between composition and mechanical properties of Mg-Al-Zn alloys by using artificial neural network. In *Materials Science Forum*; Trans Tech Publications Ltd.: Stafa-Zurich, Switzerland, 2005; Volume 488–489, pp. 793–796.
15. Mayer, A.E.; Krasnikov, V.S.; Pogorelko, V.V. Homogeneous nucleation of dislocations in copper: Theory and approximate description based on molecular dynamics and artificial neural networks. *Comput. Mater. Sci.* **2022**, *206*, 111266. [[CrossRef](#)]
16. Li, B.; Zhang, S.H.; Zhang, G.L.; Zhang, H.Y.; Zhang, H.Q. Microstructure simulation of copper tube and its application in three roll planetary rolling. *Mater. Sci. Technol.* **2007**, *23*, 715–722. [[CrossRef](#)]
17. Ertuğrul, Ö.F. A novel type of activation function in artificial neural networks: Trained activation function. *Neural Netw.* **2018**, *99*, 148–157. [[CrossRef](#)]
18. Mesbah, M.; Fattahi, A.; Bushroa, A.R.; Faraji, G.; Wong, K.Y.; Basirun, W.J.; Fallahpour, A.; Nasiri-Tabrizi, B. Experimental and Modelling Study of Ultra-Fine Grained ZK60 Magnesium Alloy with Simultaneously Improved Strength and Ductility Processed by Parallel Tubular Channel Angular Pressing. *Met. Mater. Int.* **2021**, *27*, 277–297. [[CrossRef](#)]
19. Sun, Z.; Wang, X.; Zhang, J.; Yang, H. Prediction and control of equiaxed α in near- β forging of TA15 Ti-alloy based on BP neural network: For purpose of tri-modal microstructure. *Mater. Sci. Eng. A* **2014**, *591*, 18–25. [[CrossRef](#)]
20. Li, M.; Mesbah, M.; Fallahpour, A.; Nasiri-Tabrizi, B.; Liu, B. Mechanical strength estimation of ultrafine-grained magnesium implant by neural-based predictive machine learning. *Mater. Lett.* **2021**, *305*, 130627. [[CrossRef](#)]
21. Yan, X.; Sedykh, A.; Wang, W.; Zhao, X.; Yan, B.; Zhu, H. In silico profiling nanoparticles: Predictive nanomodeling using universal nanodescriptors and various machine learning approaches. *Nanoscale* **2019**, *11*, 8352–8362. [[CrossRef](#)]
22. Zhang, J.; Yan, X.; Russo, D.P.; Zhu, H.; Yan, B. Prediction of Nano-Bio Interactions through Convolutional Neural Network Analysis of Nanostructure Images. *ACS Sustain. Chem. Eng.* **2020**, *8*, 19096–19104.
23. Mishra, A.; Chandra, P.; Ghose, U.; Sodhi, S.S. Bi-modal derivative adaptive activation function sigmoidal feedforward artificial neural networks. *Appl. Soft Comput.* **2017**, *61*, 983–994. [[CrossRef](#)]
24. Mohammed, M.A.; Naji, T.A.H.; Abduljabbar, H.M. The effect of the activation functions on the classification accuracy of satellite image by artificial neural network. *Energy Procedia* **2019**, *157*, 164–170. [[CrossRef](#)]
25. Lizhen, W.; Yifan, Z.; Gang, W.; Xiaohong, H. A novel short-term load forecasting method based on mini-batch stochastic gradient descent regression model. *Electr. Power Syst. Res.* **2022**, *211*, 108226. [[CrossRef](#)]
26. Phong, L.T.; Phuong, T.T. Differentially private stochastic gradient descent via compression and memorization. *J. Syst. Archit.* **2023**, *135*, 102819. [[CrossRef](#)]
27. Cordeiro, A.S.; Santos, S.R.d.; Moreira, F.B.; Santos, P.C.; Carro, L.; Alves, M.A.Z. Efficient Machine Learning execution with Near-Data Processing. *Microprocess. Microsyst.* **2022**, *90*, 104435. [[CrossRef](#)]
28. Huang, F.; Teng, Z.; Guo, Z.; Catani, F.; Huang, J. Uncertainties of landslide susceptibility prediction: Influences of different spatial resolutions, machine learning models and proportions of training and testing dataset. *Rock Mech. Bull.* **2023**, *2*, 100028. [[CrossRef](#)]

Disclaimer/Publisher's Note: The statements, opinions and data contained in all publications are solely those of the individual author(s) and contributor(s) and not of MDPI and/or the editor(s). MDPI and/or the editor(s) disclaim responsibility for any injury to people or property resulting from any ideas, methods, instructions or products referred to in the content.